# Non-uniform imaging (continued)

SINA 2010/11

# Logpolar mapping

$$w = f(z) = \log_a(z), \quad w, z \in C$$

$$z = x + iy = r(\cos\varphi + i\sin\varphi)$$

$$w = \rho(z) + i\,\vartheta(z)$$

$$z = re^{i\varphi}$$

$$\begin{cases} \rho = \log_a r \\ \vartheta = h\varphi \end{cases}$$

# Geometrical interpretation

$$\begin{cases} \eta = q\vartheta \\ \xi = \log_a \frac{\rho}{\rho_0} \end{cases}$$

$\rho$ and $\vartheta$ are the standard polar coordinates

$$\begin{cases} x = \rho\cos\vartheta \\ y = \rho\sin\vartheta \end{cases}$$

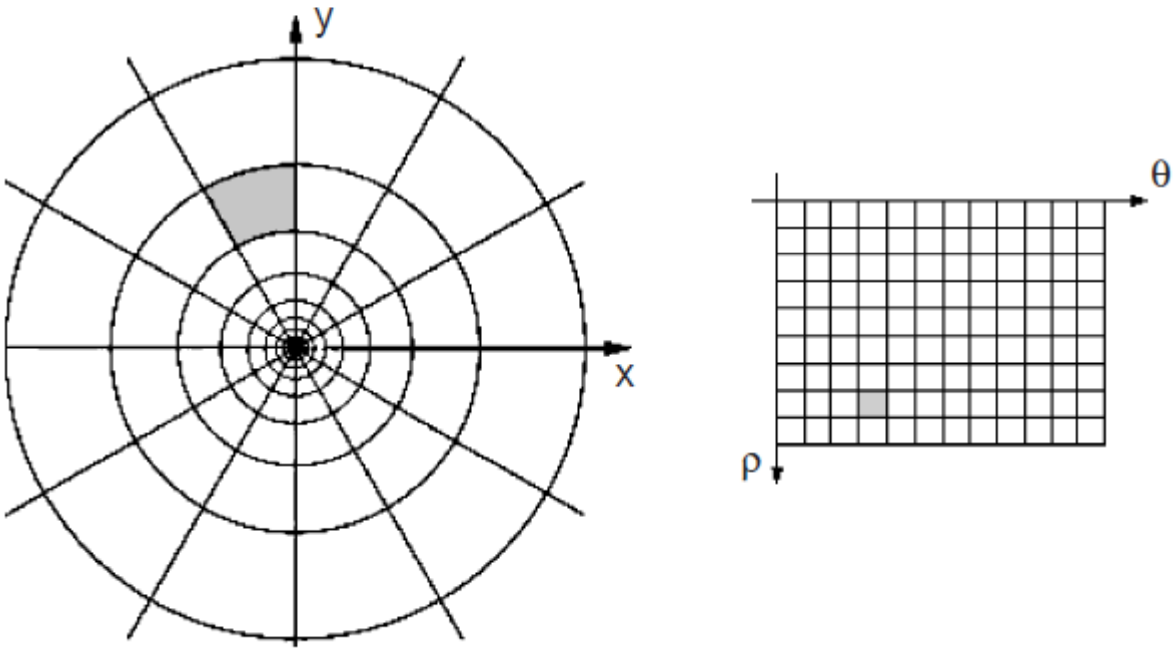


(a) (b)

# Properties

- Conformal mapping, proximity
  - Use of local operators
- Scale change
  - Translation along the real axis
- Rotation change
  - Translation along the imaginary axis
- Translations
- Fourier-Mellin Transform

# Angle preservation

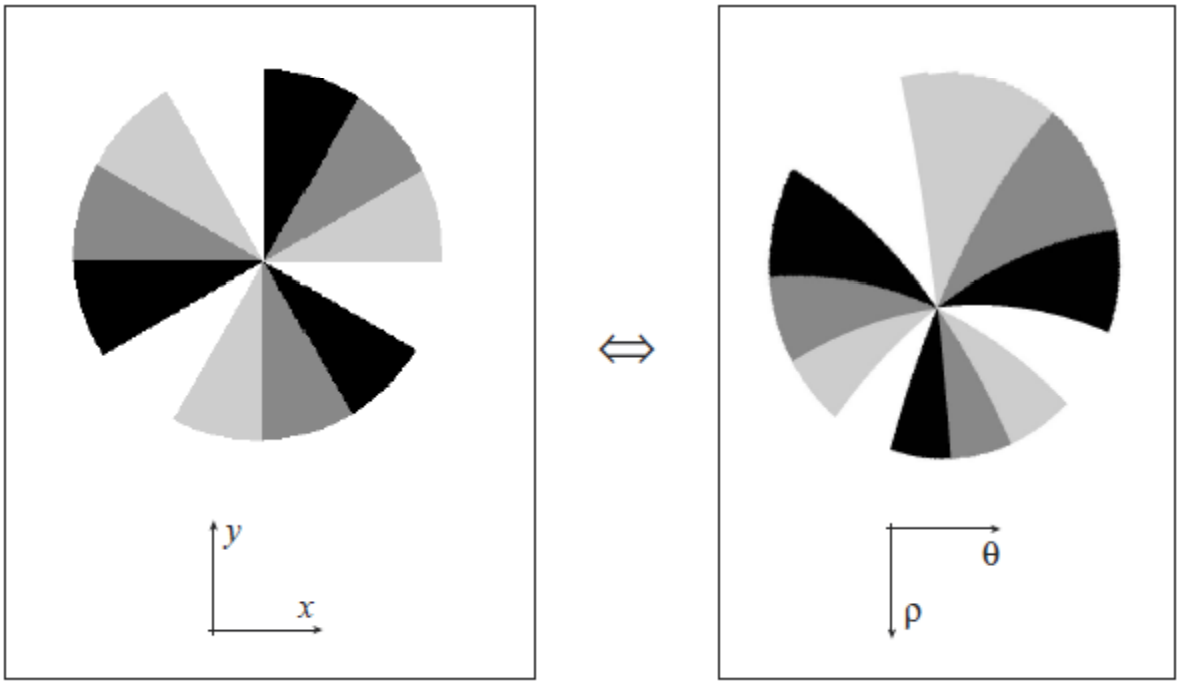


**Figure 4.1.** Angle Preservation: The angles are locally preserved after a log-polar Transformation. (a) Cartesian domain. (b) log-polar domain. Please note that both images a and b are particulars, so the origin of the mapping falls outside of the cartesian image.

# Scale

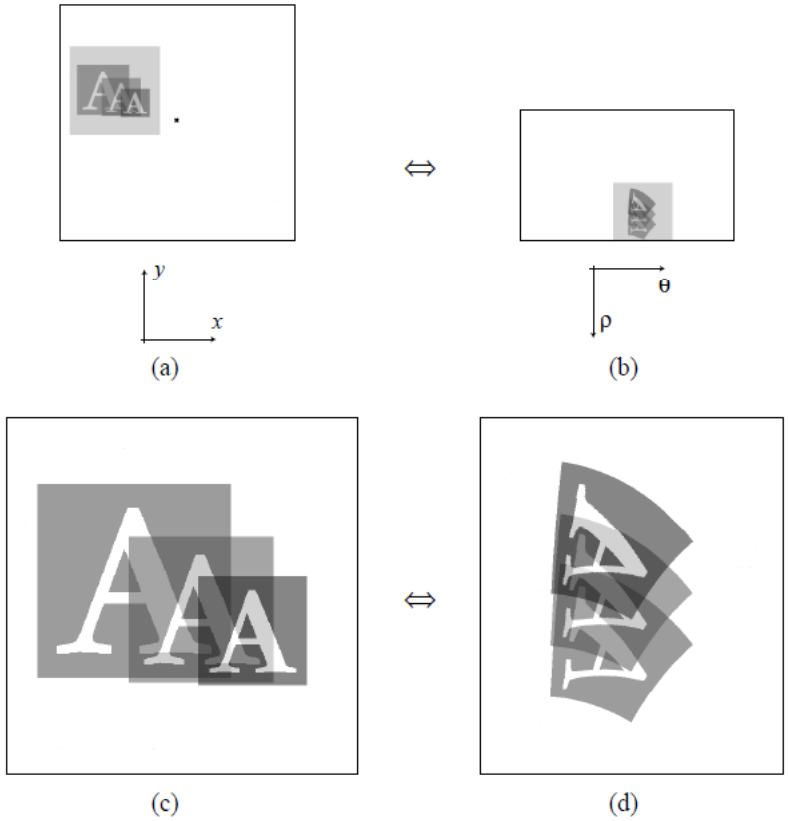


**Figure 4.2.** Scale Change: A pure scale change referred to the origin of the mapping, with no translational components, becomes a pure translation after the log-polar transform. (a) Cartesian domain. (b) log-polar domain. (c), (d) Enlargement of the shaded areas respectively in (a) and (b).

# Rotation invariance

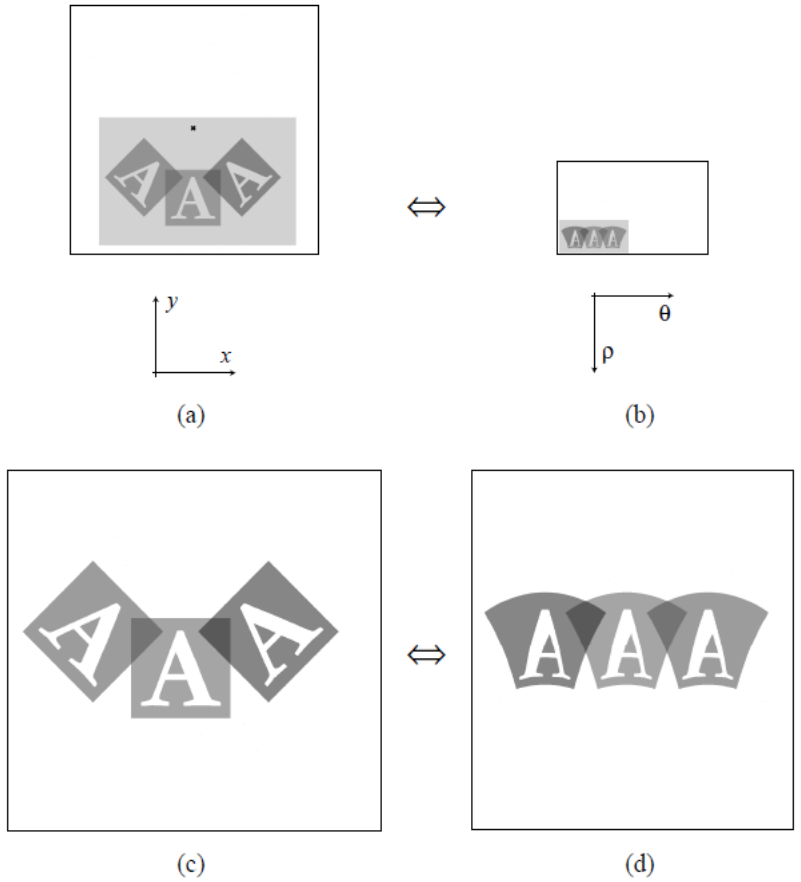


**Figure 4.3.** Rotation: A pure rotation referred to the origin of the mapping, with no translational components, becomes a pure translation after the log-polar transform. (a) Cartesian domain. (b) log-polar domain. (c), (d)Enlargement of the shaded areas respectively in (a) and (b).

# Examples of rot-scale invariance

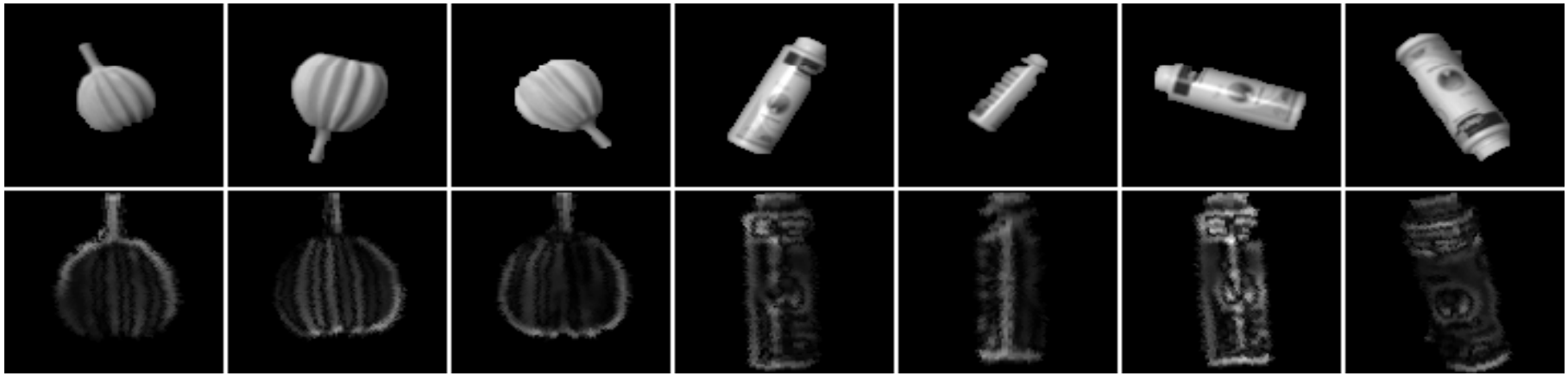

# Translations

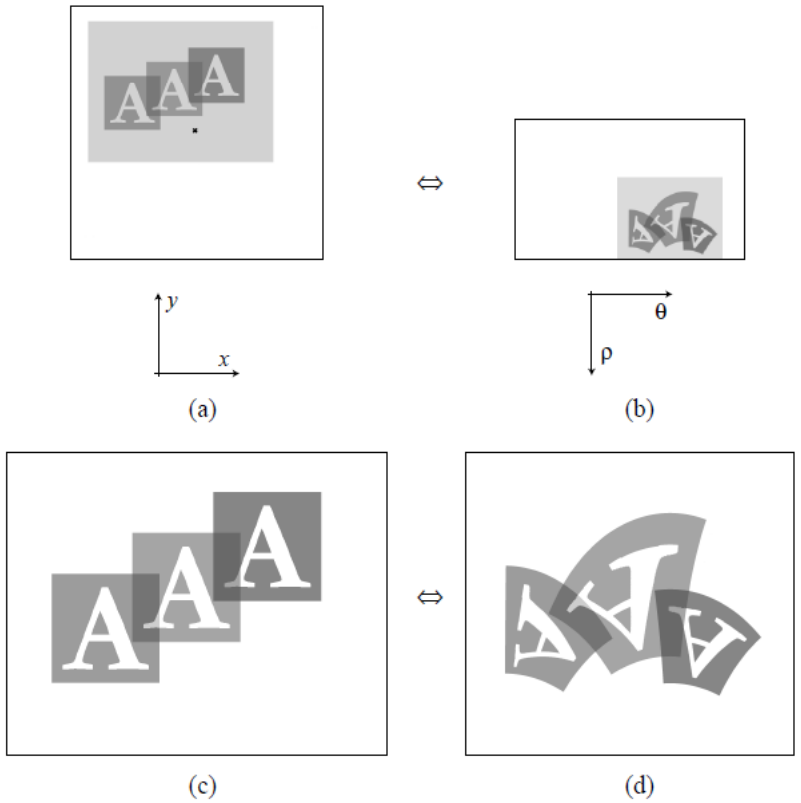


**Figure 4.4.** Translation: A pure translation implies a deformation of the object after the log-polar transform. (a) Cartesian domain. (b) log-polar domain. (c), (d) Enlargement of the shaded areas respectively in (a) and (b).

# Fourier-Mellin transform

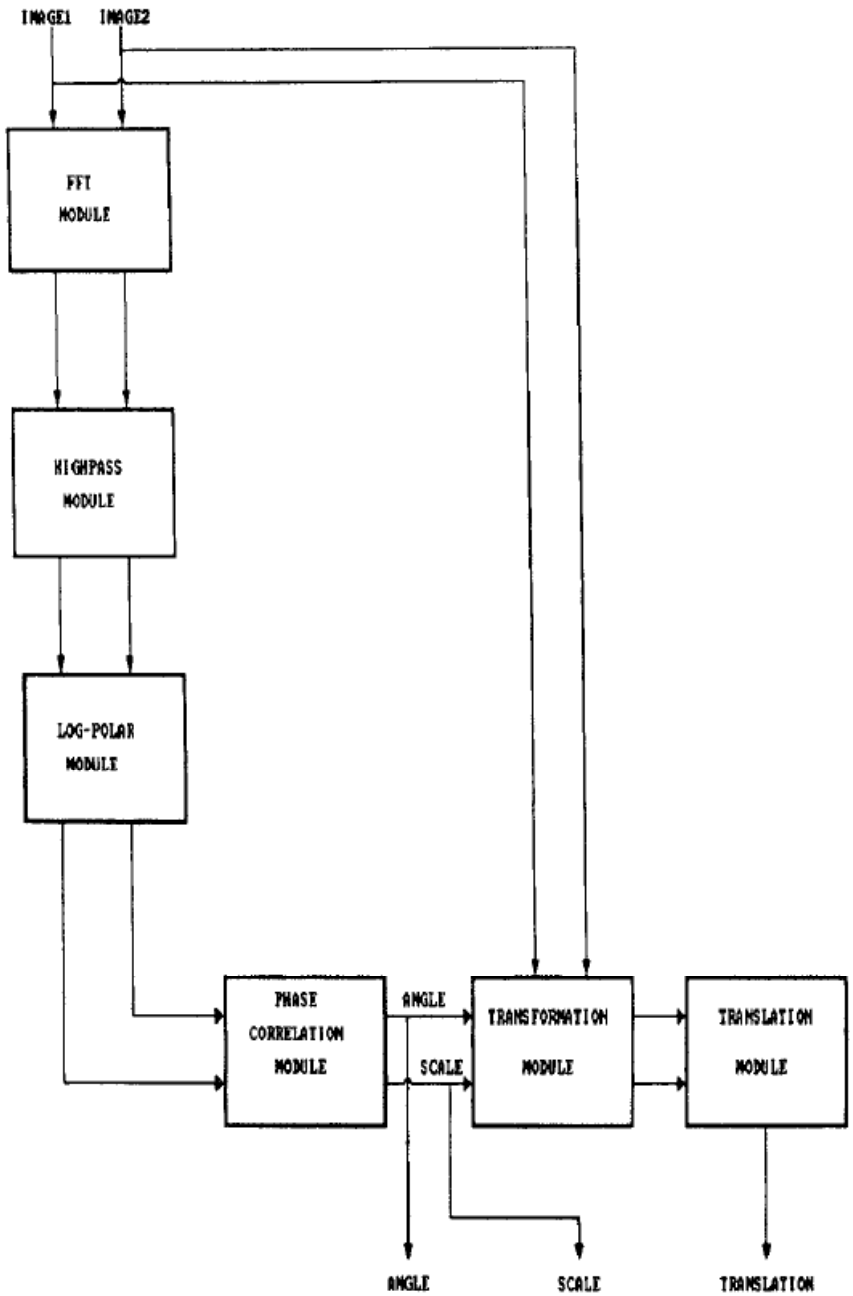


Fig. 1. Overview of the registration algorithm.

# FMT-based optical flow

(a) Frame 14

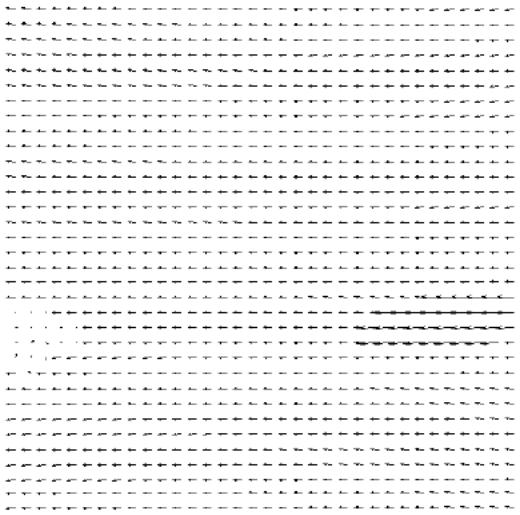

(b) Ground Truth

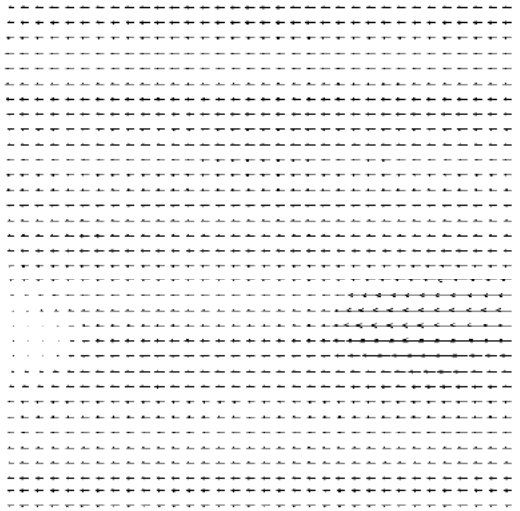

(c) Proposed FMT method

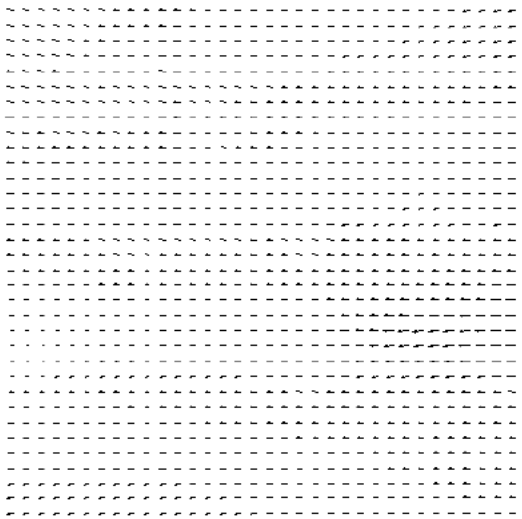

(d) Bruhn *et al.*

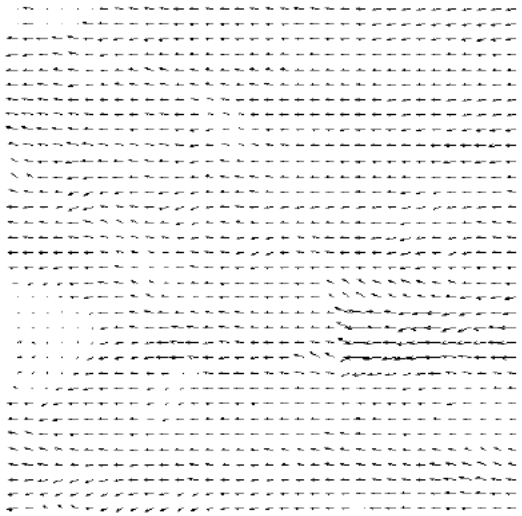

(e) Lucas-Kanade

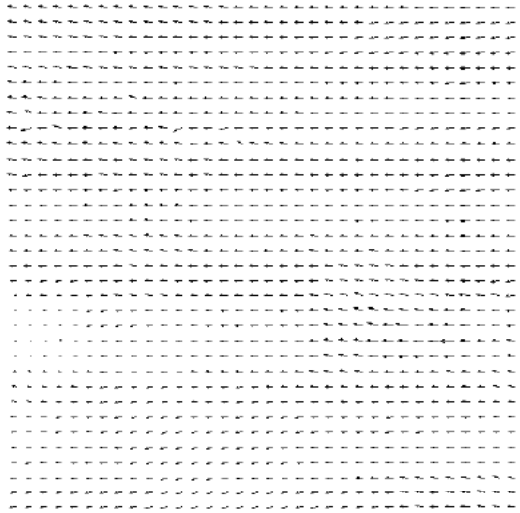

(f) Proesmans *et al.*


(a) Frame 10

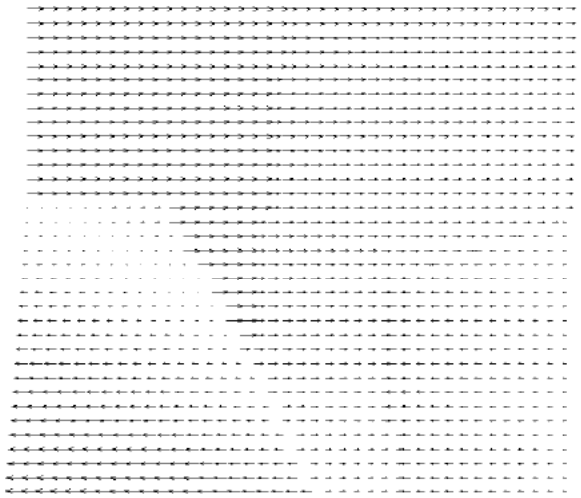

(b) Ground Truth

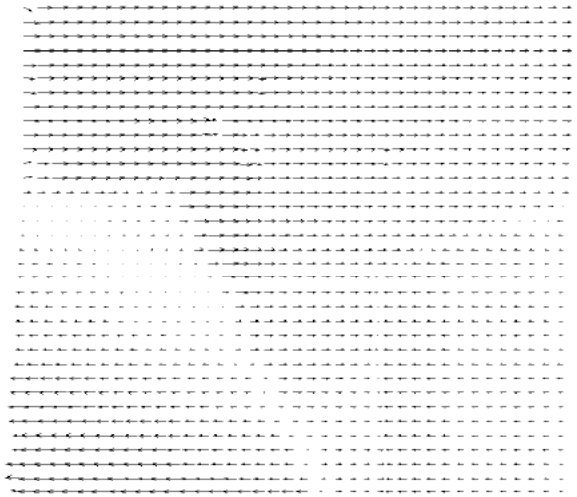

(c) Proposed FMT method

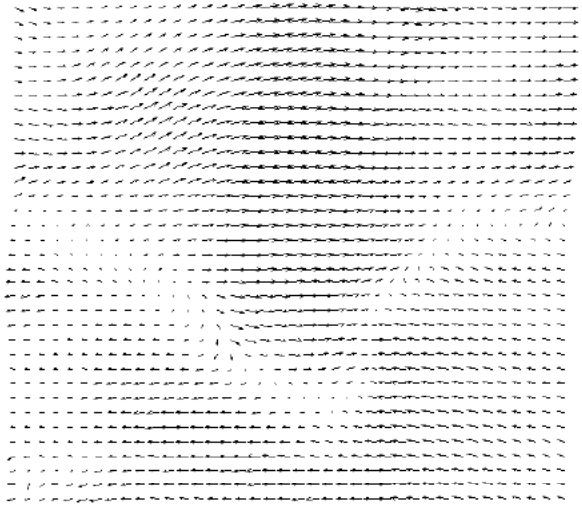

(d) Bruhn *et al.*

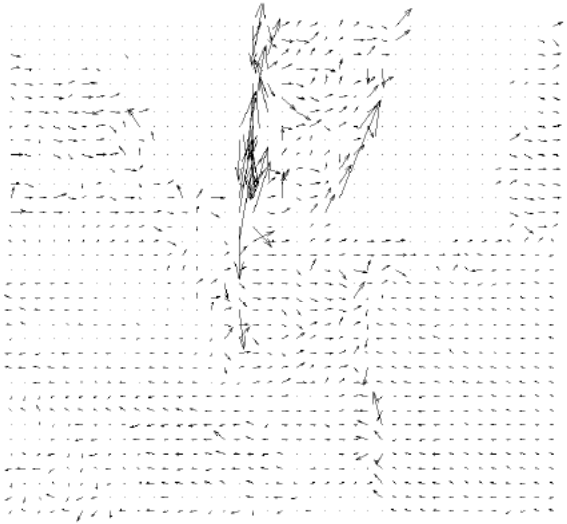

(e) Lucas-Kanade

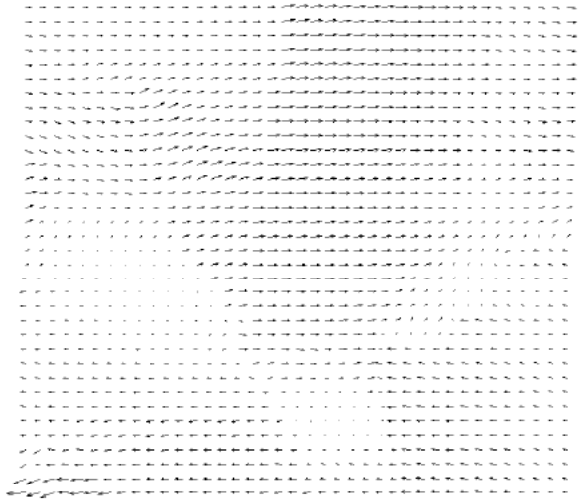

(f) Proesmans *et al.*

| Method | Street | | Venus | | RubberWhale | | Dimetrodon | | Hydrangea | |
|---|---|---|---|---|---|---|---|---|---|---|
| | $AAE$ | $AME$ | $AAE$ | $AME$ | $AAE$ | $AME$ | $AAE$ | $AME$ | $AAE$ | $AME$ |
| Lucas-Kanade | 6.45° | 0.18 | 41.27° | 0.74 | 18.69° | 0.46 | 37.14° | 0.66 | 29.85° | 0.81 |
| Proesman *et al.* | 6.31° | 0.17 | 18.25° | 0.45 | 17.43° | 0.38 | 22.23° | 0.50 | 21.49° | 0.82 |
| 2D-CLG | 4.75° | 0.15 | 19.38° | 0.45 | 16.75.° | 0.37 | 18.59° | 0.40 | 27.87° | 0.81 |
| FMT (proposed) | 4.66° | 0.14 | 5.51° | 0.14 | 10.07° | 0.26 | 7.33° | 0.18 | 11.83° | 0.56 |

Table 1: Comparison of $AAE$ and $AME$ error metrics for different methods on synthetic and real image sequences

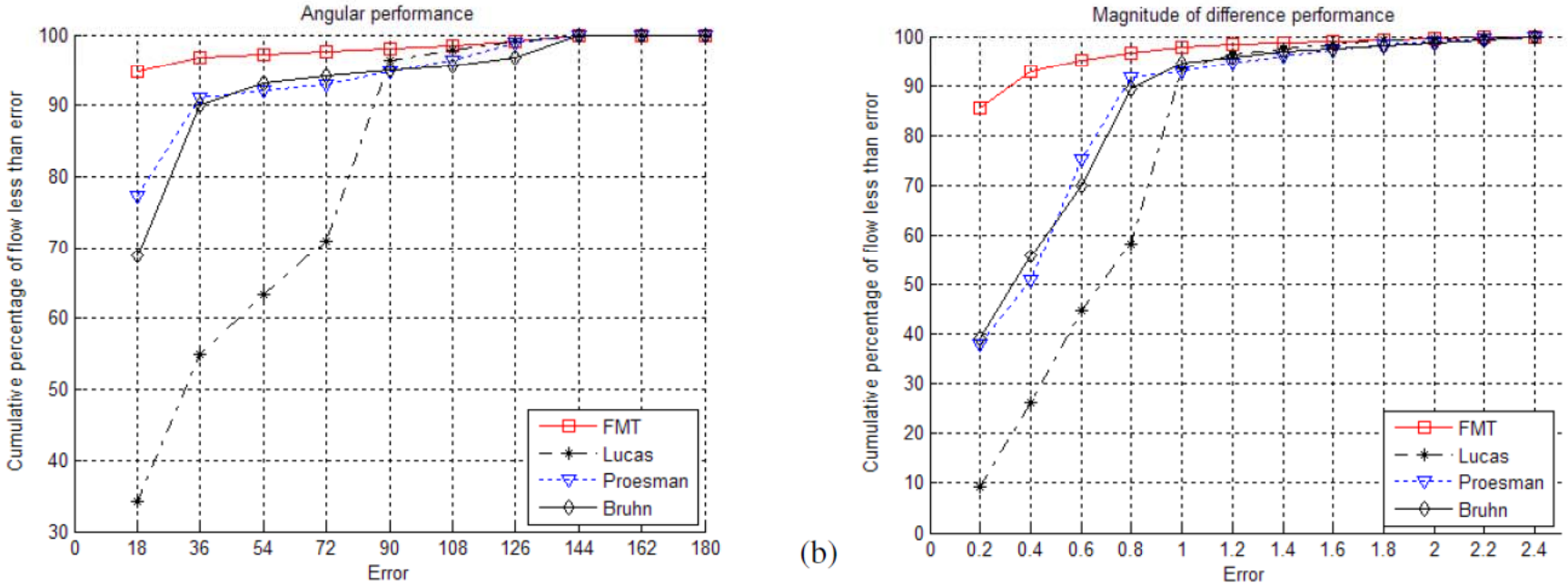


Figure 4: Performance comparison of four algorithms including the proposed FMT approach on the *Venus* sequence. Cumulative histograms for (a) average angular error and (b) average magnitude of difference error.